03,18

Recombination in gapless HgTe/CdHgTe quantum well heterostructure

© V.Ya. Aleshkin[1], A.A. Dubinov[1], V.I. Gavrilenko[1], S.G. Pavlov[2], H.-W. Hübers[2,3]

[1] Institute for Physics of Microstructures, Russian Academy of Sciences, Nizhny Novgorod, Russia
[2] Institute of Optical Sensor Systems, German Aerospace Center (DLR), Berlin, Germany
[3] Institut für Physik, Humboldt-Universitat zu Berlin, Berlin, Germany

E-mail: aleshkin@ipmras.ru

Received October 26, 2021
Revised October 26, 2021
Accepted October 28, 2021

Three recombination mechanisms of nonequilibrium carriers in gapless undoped quantum well in HgTe/CdHgTe heterostructure are considered. Dependencies of ensemble-average probability of recombination (inverse of recombination time) on concentration of nonequilibrium carriers for recombination with emission of optical phonons, recombination with emission of two-dimensional plasmons, and radiative recombination have been calculated.

Key words: gapless HgTe quantum well, recombination mechanisms of nonequilibrium carriers.

DOI: 10.21883/PSS.2022.02.54005.227

1. Introduction

Gapless quantum wells (with zero energy gap) can be used to build up detectors, mixers and to generate mid and far infrared radiation. Many suggestions were made to use graphene for these purposes (see, for example [1]). However, despite the successes in demonstration of amplification [2,3] and detection (see. for example, [4–6]) of terahertz radiation in graphene-based structures, these works did not result in creation of commercial devices. Presumably, it is related to fact that today there is no technology to produce high-quality graphene suitable to build such devices. However, gapless quantum wells can be created on the basis of HgTe/CdHgTe heterostructures as well [7], for which there are well-established production technologies [8]. Important for work of both detectors/mixers and radiation sources is the property of material known as lifetime of nonequilibrium carriers. The issue of lifetimes for graphene was studied many times experimentally (see, for example, [9] and references in it) and theoretically [10–13]. On the contrary, for gapless HgTe/CdHgTe quantum wells by now this characteristic remains almost unstudied.

The purpose of this study consists in theoretical study of recombination mechanisms and calculation of lifetime of nonequilibrium carriers in gapless HgTe/$Cd_{0.7}Hg_{0.3}Te$ quantum well. Three recombination mechanisms are considered: the recombination on optical phonons in HgTe, the recombination on plasmon-phonon modes, and the radiative recombination.

2. Electron spectrum of a gapless structure

Let us consider a HgTe quantum well with a thickness of 6.2 nm surrounded by barriers of $Cd_{0.7}Hg_{0.3}Te$. Let us assume, that it is grown on the (013) plane, because this plane is preferable for growing by the method of molecular-beam epitaxy [8]. Figure 1 shows the electron spectrum in this quantum well calculated using four-band Kane model taking into account strain effects. For details of the calculation see [14]. The lattice temperature was assumed equal to 4.2 K. For the sake of simplicity, the calculations did not take into account spin splittings of electron subbands due to the decrease in symmetry on the heterointerface and absence of center of symmetry [15], which has little to no effect on the rates of the recombination mechanisms in question.

It can be seen from Fig. 1, that at such thickness of the quantum well the structure under consideration is really a gapless structure, and the second electron band E2 is

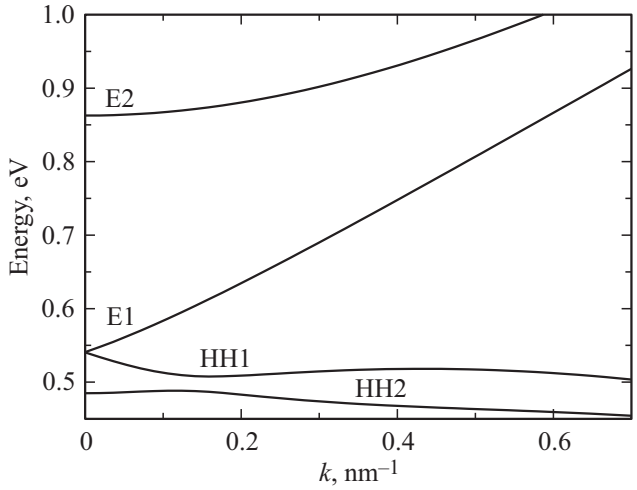

Figure 1. Electron spectrum in HgTe/$Cd_{0.7}Hg_{0.3}Te$(013) quantum well with a thickness of 6.2 nm.

located 0.321 eV above the first subband E1 in the point of $k = 0$. Since the consideration of recombination of thenonequilibrium carriers excited by the radiation quanta of far and long-wave part of mid infrared radiation with considerably lower energies is of the most interest, in the following we restrict ourselves to the the consideration of recombination processes of the E1 subband electrons and HH1 subband holes (the probability of transitions to lower hole subbands is significantly lower).

3. Recombination with involvement of bulk optical phonons in HgTe

It is well known (see, for example, [16]) that optical phonons in quantum wells can be divided into two groups: bulklike and surface phonons. In the case under consideration surface phonons are hybridized with oscillations of electron density in the quantum well — by two-dimensional plasmons. The recombination with involvement of such hybrid modes is considered in the following section. In bulklike modes the electric potential of phonons can be written as follows:

$$\varphi(\boldsymbol{\rho}, z) = \left(a_q \exp(i\mathbf{qr}) + a_q^* \exp(-i\mathbf{qr})\right)\theta(d_{QW}/2 - |z|) \times \begin{cases} \cos(\pi n z/d_{QW}), & n = 1, 3\ldots \\ \sin(\pi n z/d_{QW}), & n = 2, 4\ldots \end{cases}, \quad (1)$$

where $\mathbf{q}$ — wave vector of phonon in the plane of the quantum well, d_{QW} — width of the quantum well (the well occupies the region of $|z| < d_{QW}/2$), a_q — characterizes the potential, $\theta(z)$ — Heaviside function. By performing the procedure of secondary quantization of the optical phonons field (see Appendix), the following expression for the operator of electric potential can be derived:

$$\varphi(\boldsymbol{\rho}, z) = -A\left(c_{\mathbf{q}} \exp(i\mathbf{qr}) + c_{\mathbf{q}}^+ \exp(-i\mathbf{qr})\right)\theta\left(\frac{d_{QW}}{2} - |z|\right) \times \begin{cases} \cos(\pi n z/d_{QW}), & n = 1, 3\ldots \\ \sin(\pi n z/d_{QW}), & n = 2, 4\ldots \end{cases}, \quad (2)$$

where $c_{\mathbf{q}}^+, c_{\mathbf{q}}$ — creation and annihilation operators of the optical phonon,

$$A = \sqrt{\frac{4\pi\hbar\omega_L}{\bar{\kappa} S d_{QW}\left(q^2 + \left(\frac{\pi n}{d_{QW}}\right)^2\right)}},$$

ω_L — angular frequency of the longitudinal optical phonon, S — area of the quantum well, $\bar{\kappa}^{-1} = \kappa_\infty^{-1} - \kappa_0^{-1}$, κ_∞ and κ_0 — high-frequency and low-frequency dielectric permittivity values of the quantum well material.

Electron states in the quantum well are completely defined by setting the wave vector $\mathbf{k}$ and s index that includes the number of subband and the spin state. Thus, the electron wave function can be represented as follows:

$$\Psi_{s,\mathbf{k}}(\mathbf{r}) = S^{-1/2} \exp(i\mathbf{kr})\psi_{s,\mathbf{k}}(z). \quad (3)$$

Using (2), the following expression can be derived for the recombination probability of a hole with wave vector $-\mathbf{k}$ and index s' (the electron transits from $\mathbf{k}+\mathbf{q}, s'$ to $\mathbf{k}, s$ state):

$$w_{s,s'}(\mathbf{k}) = \frac{2\omega_L e^2}{\bar{\kappa} d_{QW}} \int d^2q \delta\left(\varepsilon_{s'}(\mathbf{k}+\mathbf{q}) - \varepsilon_s(\mathbf{k}) - \hbar\omega_L\right) \times f_{s'}(\mathbf{k}+\mathbf{q}) \sum_n \frac{|g_{s',s}(\mathbf{q}, \mathbf{k}, n)|^2}{\left(q^2 + \left(\frac{\pi n}{d_{QW}}\right)^2\right)}, \quad (4)$$

where $-e$ — electron charge, $\varepsilon_s(\mathbf{k})$ — energy of electron in the s-th state with wave vector $\mathbf{k}$, $f_s(\mathbf{k})$ — electron distribution function,

$$g_{s',s}(\mathbf{q}, \mathbf{k}, n) = \int_{-d_{QW}/2}^{d_{QW}/2} dz \psi_{s',\mathbf{k}+\mathbf{q}}^+(z)\psi_{s,\mathbf{k}}(z) \times \begin{cases} \cos(\pi n z/d_{QW}), & n = 1, 3\ldots \\ \sin(\pi n z/d_{QW}), & n = 2, 4\ldots \end{cases} \quad (5)$$

Full rate of recombination can be written as follows:

$$R = \sum_{s,s'} \frac{1}{(2\pi)^2} \int d^2k w_{s',s}(\mathbf{k})\left[1 - f_s(\mathbf{k})\right], \quad (6)$$

where s index ranges over states of the conduction band, and s' index ranges over the valence band. Note, that (6) describes full rate of recombination. The observed rate of recombination is equal to the difference between the full rate of recombination and the rate of thermal generation of carriers. We consider the case when the concentration of nonequilibrium carriers is much greater than the concentration of equilibrium carriers. In this case the thermal generation can be neglected and the ensemble-averaged probability of carrier recombination can be introduced as follows: $W = R/n$, where $n = p$ is the concentration of nonequilibrium carriers.

Figure 2 shows the results of calculations of W as a function of carriers concentration. In the calculations the concentrations of holes and electrons were assumed equal to each other, distribution functions of electrons and holes were described by Fermi-Dirac distribution with an effective electron temperature of T_e, that could be 4.2, 40, and 77 K. It can be clearly seen in the figure that there is a peak of the dependence of W on the concentration, which becomes lower and shifts to the region of high concentrations with increase in the effective temperature of nonequilibrium carriers. The decrease in W with exceedance of the concentration that corresponds to the W peak is caused by the impossibility to participate in the recombination for the electrons and holes that have kinetic energy greater than the energy of the longitudinal optical phonon. When the concentration corresponding to the peak is exceeded, the part of these carriers increases and, therefore, W decreases. The decrease in W with the decrease in concentration

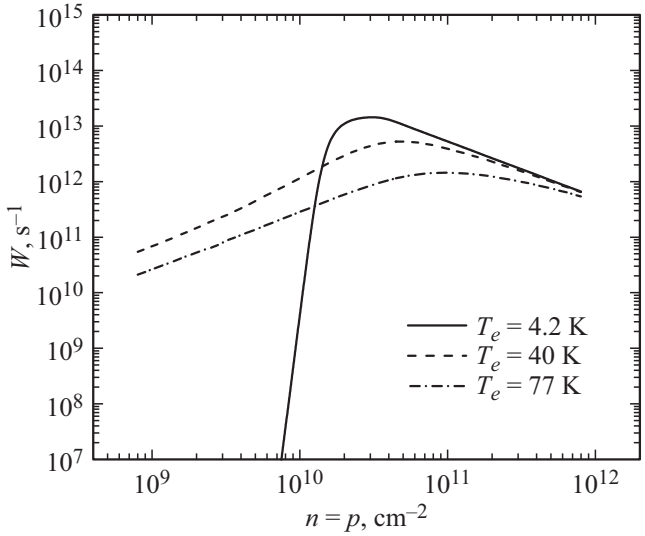

Figure 2. The ensemble-averaged probability of hole recombination on a bulklike phonon as a function of carriers concentration for three effective temperatures of nonequilibrium carriers.

of carriers in the region where the concentration is less than that corresponding to the W peak is related to the decrease in the number of electron-hole pairs involved in the recombination, when the difference of Fermi energies of electrons and holes becomes less than the energy of the optical phonon. It should be noted, that for an electron-hole pair which kinetic energy is less than the energy of optical phonon, the recombination process in question is prohibited by the energy conservation law.

4. Recombination with involvement of the plasmon-phonon mode

Nonequilibrium carriers in gapless HgTe quantum wells can recombine with emission of two-dimensional plasmons. In [17] the recombination with involvement of two-dimensional plasmons in a narrow-gap quantum well was studied, however, the case of gapless quantum well was not considered.

The interaction of two-dimensional plasmons with optical phonons of barrier layers (it is assumed that quantum well width is much less than the wave length of plasmon) results in formation of high-frequency and low-frequency plasmon-phonon modes, in a similar way as it takes place in a bulk semiconductor [18]. Frequency of the high-frequency mode exceeds the frequency of longitudinal optical phonon in the barrier, and frequency of the low-frequency mode is less than the frequency of transverse optical phonon in the barrier. The plasmon-phonon modes like these are surface optical oscillations of the lattice concentrated near the boundaries of the quantum well.

Figure 3 shows dependencies of plasmon-phonon excitation energy on the wave vector at different concentrations of carriers. To determine the dependency of plasmon-phonon modes frequency on the wave vector, the technique was used, which detailed description can be found in [19]. The „end“ points of dispersion laws of plasmon-phonon modes are caused by „switching on“ of the Landau damping, that makes these modes poorly defined due to large losses. In the conditions of Landau damping, the imaginary component of the plasmon frequency becomes of the order of magnitude of its real component, and damping time of these plasmons becomes much less that the typical recombination time. Thus, in the conditions of Landau damping the contribution of plasmons in the recombination is insignificant. Therefore, only the contribution of plasmons in the recombination was taken into account, which have no Landau damping.

The effective temperature of electron and hole gas in the calculations had three values: 4.2, 40, and 77 K. Note, that increase in the effective temperature of charge carriers has little effect on the dispersion law of the plasmons under consideration [19], however, it decreases the wave vector at which the Landau damping becomes significant.

Electric field of a plasmon has two components: one of them is directed along the wave vector, and another is normal to the quantum well (along the z axis). The component that is directed along the wave vector is an even function of z, if the point of origin is selected in the middle of the quantum well. Since the typical scale of its variation in the direction of z is $1/q$, and width of the quantum well is assumed much less than $1/q$, this component can be considered constant within the quantum well. Another component of electric field is an odd function of z. At the boundaries of the quantum well these component are nearly equal to each other in magnitude. Therefore, the probability of electron transition from the conduction band to the valence band of the quantum well under the action of the plasmon electric field is higher for the component of

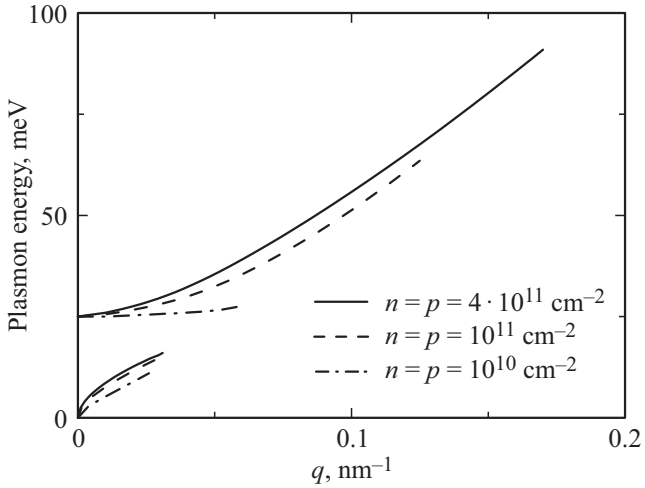

Figure 3. Quantum energies of plasmon-phonon modes as functions of the wave vector for three concentrations of nonequilibrium carriers. $T_e = 4.2$ K.

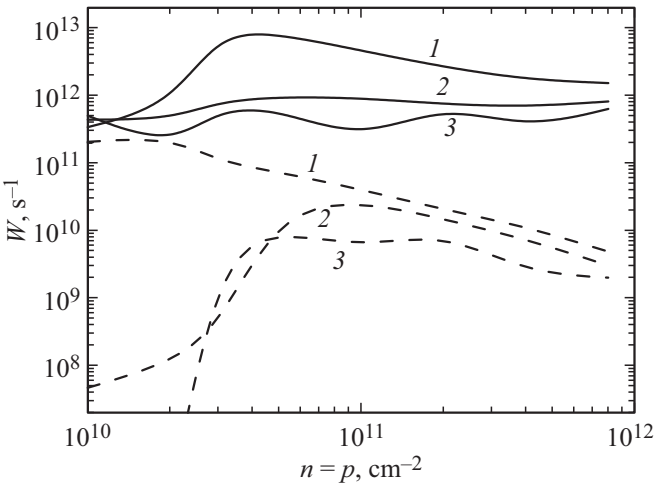

Figure 4. The probability of recombination with plasmon-phonon mode quantum emission as a function of nonequilibrium carriers concentration (solid lines). Dashed lines represent the probability of recombination with emission of low-frequency plasmon-phonon mode quantum. Figures 1, 2, 3 correspond to $T_e = 4.2\,\mathrm{K}$, $T_e = 40\,\mathrm{K}$ and $T_e = 77\,\mathrm{K}$.

the electric field laying in the plane of the quantum well. To determine the probability of these transitions, we can use the operator of vector-potential component directed along the wave vector, as presented in [17]:

$$\mathbf{A}_{\parallel} = -c \sum_{\mathbf{q},j} \frac{\mathbf{q}}{\omega} \sqrt{\frac{2\hbar}{Sq^2} \left(\frac{\partial \chi(\mathbf{q},\omega)}{\partial \omega} \right)^{-1}} \times \left(d_{\mathbf{q},j} \exp(i\mathbf{qr} - i\omega t) + d^{+}_{\mathbf{q},j} \exp(-i\mathbf{qr} + i\omega t) \right), \quad (7)$$

where $\chi(\mathbf{q},\omega)$ — polarizability of electron-hole two-dimensional gas (the expression to calculate the $\chi(\mathbf{q},\omega)$ can be found in [17]), $d^{+}_{\mathbf{q}}$ and $d_{\mathbf{q}}$ — operators of creation and annihilation of plasmon-phonon mode quantum, j index is introduced to denote high-frequency and low-frequency mode. With the use of (7), the following expression for the rate of recombination with plasmon emission can be derived:

$$R = \frac{2}{(2\pi)^3} \sum_{j,s,s'} \int d^2k d^2q \frac{|\mathbf{v}_{s,\mathbf{k};s',\mathbf{k}+\mathbf{q}}\mathbf{q}|^2}{q^2 \omega_j^2(\mathbf{q})} \left(\frac{\partial \chi(\mathbf{q},\omega_j)}{\partial \omega_j} \right)^{-1} \times \delta\left(\varepsilon_s(\mathbf{k}) - \varepsilon_{s'}(\mathbf{k}+\mathbf{q}) - \hbar\omega_j(\mathbf{q})\right)\left(1 - f_{s'}(\mathbf{k}+\mathbf{q})\right) f_s(\mathbf{k}), \quad (8)$$

where $\mathbf{v}_{s,\mathbf{k};s',\mathbf{k}+\mathbf{q}}$ — matrix element of the speed operator, s index ranges over states of the conduction band, while s' index ranges over states of the valence band.

Figure 4 shows dependencies of the ensemble-averaged probability of recombination with emission of plasmon-phonon mode quanta $W = R/n$. Solid lines represent the sum recombination including emission of quanta of high-frequency and low-frequency modes. Dashed lines represent emission of low-frequency mode quanta only. It can be seen from the figure, that the main role if the recombination mechanism under consideration is played by the processes with emission of high-frequency mode quanta. An exception from this statement is the case when $T_e = 4.2\,\mathrm{K}$ and the concentration of nonequilibrium carriers is less than $2 \cdot 10^{10}\,\mathrm{cm}^{-2}$. It can be clearly seen from the figure, that the probability of recombination is a nonmonotone function of the concentration of nonequilibrium carriers and that its magnitude decreases with increase in the effective temperature of carriers.

5. Radiative recombination

This mechanism is the slowest among the recombination mechanisms under consideration, and it is considered here mainly for illustration and comparison purposes. It should be noted, that the radiative recombination in the solid solution of $Cd_xHg_{1-x}Te$ was studied in [20].

The probability of spontaneous electron transition with a wave vector of $\mathbf{k}$ with emission of photon from the conduction band state s to unoccupied state of the valence band s' is equal to:

$$w_{s',s}(\mathbf{k}) = \frac{4\sqrt{\kappa}e^2\omega}{3\hbar c^3} |\mathbf{v}_{s',s}(\mathbf{k})|^2, \quad (9)$$

where $\mathbf{v}_{s',s}(\mathbf{k}) = \mathbf{v}_{s,\mathbf{k};s',\mathbf{k}}$. A reciprocal of radiative time of recombination (frequency of radiative recombination) is equal to the ratio between the radiative recombination rate and the concentration of minority carriers. For n-type semiconductor or in the case of $n = p$, it can be written as follows [21]:

$$W = \frac{\sum\limits_{s,s'} \int d^2k w_{s,s'}(\mathbf{k}) f_s(\mathbf{k}) \left(1 - f_{s'}(\mathbf{k})\right)}{\sum\limits_{s} \int d^2k f_s(\mathbf{k})}. \quad (10)$$

Figure 5 shows calculated dependencies $w(n)$ for three effective temperatures of nonequilibrium carriers.

It can be seen from the figure, that there is a peak of $W(n)$ dependence at $T_e = 4.2\,\mathrm{K}$, which is caused by filling of side extremums by holes (see Fig. 1) with increase in concentration of nonequilibrium carriers. Holes in the side extremums are not involved in the radiative recombination, because there are no electrons in the conduction band with wave vectors corresponding to the side extremums. By comparing Figures 2, 4, and 5, it can be seen that the radiative recombination is the slowest among the recombination mechanisms under consideration.

6. Conclusion

In the conclusion the main results of the study are described. Dependencies of recombination probability on concentration of nonequilibrium carriers in the gapless HgTe quantum well are calculated for three mechanisms of recombination: the recombination with emission of

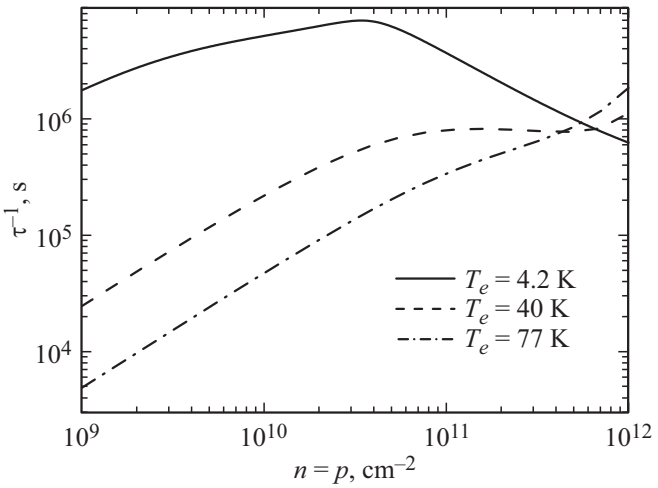

Figure 5. Dependence of $W(n)$ for radiative recombination for three effective temperatures.

optical phonons, the recombination with emission of two-dimensional plasmons, and the radiative recombination. It is shown that the most effective recombination mechanisms are the recombination with emission of optical phonons and the recombination with emission of two-dimensional plasmons. Maximum probabilities of recombination for these two mechanisms have an order of magnitude of $10^{13}\,\mathrm{s}^{-1}$. Such short times of radiationless mechanisms of recombination of nonequilibrium carriers indicate non-prospectivity of the use of gapless quantum wells to generate photons and perhaps plasmons. For these purposes, more prospective are quantum wells with a gap greater than the energy of optical phonon.

Appendix

Quantization of optical phonons in a quantum well

The energy of longitudinal oscillations of the lattice can be written as follows:

$$\sum_j \bar{M}\mathbf{r}_j^2/2 + \bar{M}\omega_L^2\mathbf{r}_j^2/2 = \frac{\bar{M}}{2a^3}\int dz \int dxdy\left(\mathbf{v}\mathbf{r}^2(x,y,z) + \omega_L^2\mathbf{r}^2(x,y,z)\right), \quad (1A)$$

where $\mathbf{r}_j$ — relative displacement of atoms in the j-th unit cell, $\bar{M}$ — reduced mass of the unit cell, a^3 — volume of the unit cell. Since the wave length of optical phonons under consideration is much greater than the lattice spacing, then instead of $\mathbf{r}_j$ we can introduce the $\mathbf{r}(x,y,z)$ function, that can be considered as a function of continuous argument. In longitudinal oscillations the displacement vector is related to the electric field acting on the ion [18]:

$$\mathbf{r} = \frac{e^*\mathbf{E}}{\bar{M}(\omega_T^2 - \omega_L^2)}, \quad (2A)$$

ω_T — angular frequency of optical oscillations, e^* — effective charge of ion [18]:

$$e^* = \kappa_\infty\omega_L\sqrt{\frac{\bar{M}a^3}{4\pi\bar{\kappa}}}. \quad (3A)$$

Using (1) to determine the electric field and (2A), we can derive expressions for components of the vector $\mathbf{r}$ laying in the plane of the quantum well and z-component

$$\begin{aligned}(\mathbf{r}_\parallel(\boldsymbol{\rho},z) = &-i\mathbf{q}\big(b_\mathbf{q}\exp(i\mathbf{q}\mathbf{r} - i\omega t)\\ &- b_\mathbf{q}^*\exp(-i\mathbf{q}\mathbf{r} + i\omega t)\big)\theta(d_{QW}/2 - |z|)\\ &\times\begin{cases}\cos(\pi nz/d_{QW}), & n = 1,3\ldots\\ \sin(\pi nz/d_{QW}), & n = 2,4\ldots\end{cases}\end{aligned} \quad (4A)$$

$$\begin{aligned}r_z(\boldsymbol{\rho},z) = &\frac{\pi n}{d_{QW}}\big(b_\mathbf{q}\exp(i\mathbf{q}\mathbf{r} - i\omega t)\\ &+ b_\mathbf{q}^*\exp(-i\mathbf{q}\mathbf{r} + i\omega t)\big)\theta(d_{QW}/2 - |z|)\\ &\times\begin{cases}-\sin(\pi nz/d_{QW}), & n = 1,3\ldots\\ \cos(\pi nz/d_{QW}), & n = 2,4\ldots\end{cases}\end{aligned} \quad (5A)$$

where

$$b_\mathbf{q} = -\frac{a_\mathbf{q}}{\omega_L}\sqrt{\frac{a^3\bar{\kappa}}{4\pi\bar{M}}}. \quad (6A)$$

Using (4A) and (5A), from (2A) we get an expression for the full energy of oscillations with different values of $\mathbf{q}$:

$$\frac{\bar{M}}{a^3}\omega_L^2 S d_{QW}\sum_\mathbf{q} b_\mathbf{q}b_\mathbf{q}^*\left(q^2 + \left(\frac{\pi n}{d_{QW}}\right)^2\right). \quad (7A)$$

Let us introduce canonical variables of field:

$$Q_\mathbf{q} = \sqrt{A}(b_\mathbf{q} + b_\mathbf{q}^*),\ P_\mathbf{q} = -i\omega\sqrt{A}(b_\mathbf{q} - b_\mathbf{q}^*), \quad (8A)$$

where

$$A = \frac{1}{2}\frac{\bar{M}}{\Omega}Sd_{QW}\left(q^2 + \left(\frac{\pi n}{d_{QW}}\right)^2\right).$$

In this case (7A) can be written as: $\frac{1}{2}\sum_q P_\mathbf{q}^2 + \omega_L^2 Q_\mathbf{q}^2$. Following the standard procedure, let us introduce operators for creation and annihilation of phonon:

$$c_\mathbf{q}^+ = \sqrt{\frac{\omega}{2\hbar}}\left(Q_\mathbf{q} - \frac{iP_\mathbf{q}}{\omega}\right),\ c_\mathbf{q} = \sqrt{\frac{\omega}{2\hbar}}\left(Q_\mathbf{q} + \frac{iP_\mathbf{q}}{\omega}\right). \quad (9A)$$

Using (1), (6A), (8A), and (9A), we get an expression for operator (2).

Funding

This research work was financially supported by the co-project of RFBR (RFBR-Deutsche Forschungsgemeinschaft grant_a No. 21-52-12020) and Deutsche Forschungsgemeinschaft (DFG Project 448961446).

Conflict of interest

The authors declare that they have no conflict of interest.

References

[1] K.S. Novoselov, A.K. Geim, S.V. Morozov, D. Jiang, M.I. Katsnelson, I.V. Grigorieva, S.V. Dubonos, A.A. Firsov. Nature, **438**, 197 (2005).
[2] D. Yadav, G. Tamamushi, T. Watanabe, J. Mitsushio, Y. Tobah, K. Sugawara, A.A. Dubinov, A. Satou, M. Ryzhii, V. Ryzhii, T. Otsuji. Nanophotonics **7**, 741 (2018).
[3] S. Boubanga-Tombet, W. Knap, D. Yadav, A. Satou, D.B. But, V.V. Popov, I.V. Gorbenko, V. Kachorovskii, T. Otsuji. Phys. Rev. X, **10**, 031004 (2020).
[4] L. Vicarelli, M.S. Vitiello, D. Coquillat, A. Lombardo, A.C. Ferrari, W. Knap, M. Polini, V. Pellegrini, A. Tredicucci. Nature Mater. **11**, 865 (2012).
[5] X. Cai, A.B. Sushkov, R.J. Suess, M. M. Jadidi, G.S. Jenkins, L.O. Nyakiti, R.L. Myers-Ward, S. Li, J. Yan, D.K. Gaskill, T.E. Murphy, H.D. Drew, M. S. Fuhrer. Nature Nanotechnology **9**, 814 (2014).
[6] D.A. Bandurin, D. Svintsov, I. Gayduchenko, S.G. Xu, A. Principi, M. Moskotin, I. Tretyakov, D. Yagodkin, S. Zhukov, T. Taniguchi, K. Watanabe, I.V. Grigorieva, M. Polini, G.N. Goltsman, A.K. Geim G. Fedorov. Nature Commun. **9**, 5392 (2018).
[7] B. Buttner, C.X. Liu, G. Tkachov, E.G. Novik, C. Brune, H. Buhmann, E.M. Hankiewicz, P. Recher, B. Trauzettel, S.C. Zhang, L.W. Molenkamp. Nature Phys. **7**, 418 (2011).
[8] S. Dvoretsky, N. Mikhailov, Yu. Sidorov, V. Shvets, S. Danilov, B. Wittman. J. Electron. Mater. **39**, 918 (2010).
[9] P. Huang, E. Riccardi, S. Messelot, H. Graef, F. Valmorra, J. Tignon, T. Taniguchi, K. Watanabe, S. Dhillon, B. Plaçais, R. Ferreira, J. Mangeney. Nature Commun. **11**, 863 (2020).
[10] F. Rana. Phys. Rev. B **76**, 155431 (2007).
[11] F. Rana, P.A. George, J.H. Strait, J. Dawlaty, S. Shivaraman, M. Chandrashekhar, M.G. Spencer. Phys. Rev. B **79**, 115447 (2009).
[12] F. Rana, J.H. Strait, H. Wang, C. Manolatou. Phys. Rev. B, **84**, 045437 (2011).
[13] G. Alymov, V. Vyurkov, V. Ryzhii, A. Satou, D. Svintsov. Phys. Rev. B, **97**, 205411 (2018).
[14] M.S. Zholudev, A.V. Ikonnikov, F. Teppe, M. Orlita, K.V. Maremyanin, K.E. Spirin, V.I. Gavrilenko, W. Knap, S.A. Dvoretskiy, N.N. Mihailov. Nanoscale Res. Lett. **7**, 534 (2012).
[15] S.A. Tarasenko, M.V. Durnev, M.O. Nestoklon, E.L. Ivchenko, J.-W. Luo, A. Zunger. Phys. Rev. B **91**, 081302(R) (2015).
[16] K. Huang, B. Zhu. Phys. Rev. B **38**, 13377 (1988).
[17] V.Ya. Aleshkin, G. Alymov, A.A. Dubinov, V.I. Gavrilenko, F. Teppe. J. Phys. Commun. **4**, 115012 (2020).
[18] P. Yu, M. Kardona, Fundamentals of semiconductor physics, Fizmatlit, M, (2002) (in Russian).
[19] V.Ya. Aleshkin, A.A. Dubinov, V.I. Gavrilenko, F. Teppe. J. Opt., **23**, 115001 (2021).
[20] N.L. Bazhenov, K.D. Mynbayev, G.G. Zegrya, Physics and Technique of Semiconductors, **49**, 1206 (2015) (in Russian).
[21] V.Ya. Aleshkin, A.A. Dubinov, V.V. Rumyantsev, M.A. Fadeev, O.L. Domnina, N.N. Mikhailov, S.A. Dvoretsky, F. Teppe, V.I. Gavrilenko, S.V. Morozov. J. Phys.: Condens. Matter **30**, 495301 (2018).